Supplementary Materials for "Ising model for melt ponds on Arctic sea ice"

Spatial scale from snow topography data. — The lattice constant a must be small relative to the 10-20 m length scales prominent in sea ice and snow topography [35]. We set $a = 1$ m as the length above which the power spectral density (psd) of observed snow topography exceeds a null red noise spectrum (Supplementary Fig. 1). For this calculation, we used 13 radar transects collected during the Surface Heat Budget of the Arctic Ocean (SHEBA) project [36]. To estimate the psd via the Welch modified periodogram, we calculated the power spectrum for each transect with a Hanning window and 50% segment overlap, and then averaged the results across the transects. We calculated the corresponding null red noise spectrum based on lag-one spatial autocorrelation [37] averaged across the transects.

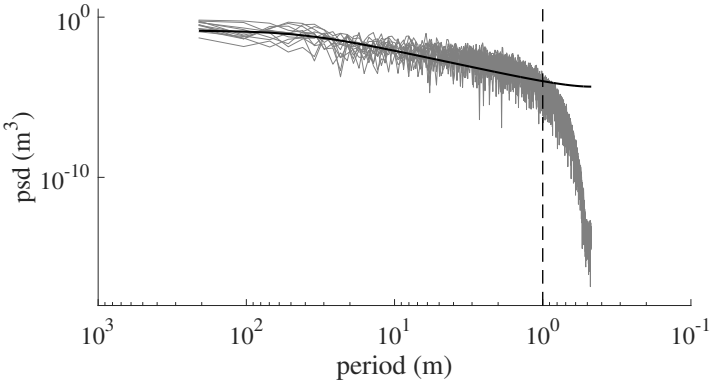

Supplementary Figure 1. Snow depth power spectral density (gray curve) with corresponding null red noise spectrum (black curve). The lattice constant $a = 1$ m is indicated by a vertical dashed line.

Temporal scale from vertical energy balance. — The melt pond system can be modeled as a thin active layer on top of the bulk sea ice floe, subject to incoming and outgoing radiation and heat exchange with the bulk. Let R_+ be the net radiation received by water, and R_- be the net radiation received by ice:

$$R_+ = \mathrm{ISR}_+ - \mathrm{OLR}, \quad R_- = \mathrm{ISR}_- - \mathrm{OLR}, \tag{S1}$$

where ISR and OLR respectively represent the incoming shortwave radiation and the outgoing longwave radiation. The former is $\mathrm{ISR}_+ = Q(1-\alpha_+)$ and $\mathrm{ISR}_- = Q(1-\alpha_-)$, where $Q = 460\ \mathrm{W \cdot m^{-2}}$ is the mean solar insolation during polar summer, and α is the surface albedo with $\alpha_+ = 0.1$ for water and $\alpha_- = 0.5$ for ice. The latter is $\mathrm{OLR} = \sigma(T + 273)^4$, where $\sigma = 5.67 \times 10^{-8}\ \mathrm{W \cdot m^{-2} K^{-4}}$ is the Stefan-Boltzmann constant, and the temperature $T \approx 0$ Celsius for both water and ice. Therefore we obtain $R_+ = 99\ \mathrm{W \cdot m^{-2}}$ and $R_- = -85\ \mathrm{W \cdot m^{-2}}$.

Bulk sea ice as a porous composite of brine and ice on the microscopic scale often has a temperature just below zero Celsius during the melt season. Meanwhile, the heat transfer between the bulk sea ice and the active layer of melt ponds is known to be very efficient. As a result, a patch of water in the active layer always has a temperature

slightly above zero Celsius due to the positivity of R_+, and a patch of ice in the active layer always has a temperature slightly below zero Celsius due to the negativity of R_-.

If external influences such as surface topography and interactions with the surroundings are present, a patch of water in the active layer can transition into ice, and vice versa. We assume that the transition of a patch of water to ice is facilitated by changing the net radiation from R_+ to R_-, and that the transition of a patch of ice to water is facilitated by changing the net radiation from R_- to R_+. The required energies per unit area to freeze water and to melt ice are respectively $E_+ = -L\rho_+ h$ and $E_- = L\rho_- h$, where $L = 3.34 \times 10^5\ \mathrm{J \cdot kg^{-1}}$ is the latent heat of fusion, $\rho_+ = 1 \times 10^3\ \mathrm{kg \cdot m^{-3}}$ is the density of water, $\rho_- = 9.2 \times 10^2\ \mathrm{kg \cdot m^{-3}}$ is the density of ice, and $h = 0.1$ m is a realistic value for the height of the active layer. Therefore, the time scales required to freeze water and to melt ice under these assumptions are respectively $\tau_{w\to i} = E_+/R_- = 5$ days and $\tau_{i\to w} = E_-/R_+ = 4$ days. For example, this rough estimate gives a time scale of about 20 days, or 4 steps of spin flipping, for a well-developed network of ponds like those in Fig. 4(b) to evolve, which is reasonable.

Alternative quantifier of the onset of complexity. — To account for the entire cluster of points in the (A, P)-plane in Fig. 3(a), we define a new quantifier of the onset of complexity as the variance σ of $\log(P)$, hereafter referred to as the *elasticity*. As shown in Supplementary Fig. 2, there exists a critical area A_c such that $\sigma(\log(P))$ increases with $\log(A)$ for simple ponds with $A < A_c$, and decreases with $\log(A)$ for complex ponds with $A > A_c$. The onset of complexity may then be identified with maximum elasticity, which occurs at $A_c a^2 \approx 90\ \mathrm{m}^2$. This coincides with the critical area determined from Fig. 3(c) by the inflection point in the best fit.

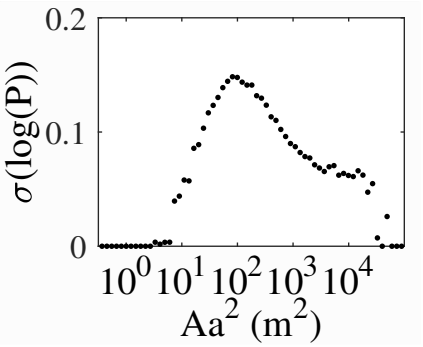

Supplementary Figure 2. Plot of the variance $\sigma(\log(P))$ as a function of A (log scale), with bin size 0.2. The maximum occurs at $A_c a^2 \approx 90\ \mathrm{m}^2$.

Percolation threshold and correlation length exponent. — For a two dimensional square lattice with occupation probability p, the site-site correlation function $g(r_i, r_j)$ gives the probability that a site at r_j is a member of the same cluster as a site at r_i. The function g is assumed to decay with large distance $d = |r_i - r_j|$ according to

$$g(d) \sim \exp\left(-\frac{d}{\xi(p)}\right), \tag{S2}$$

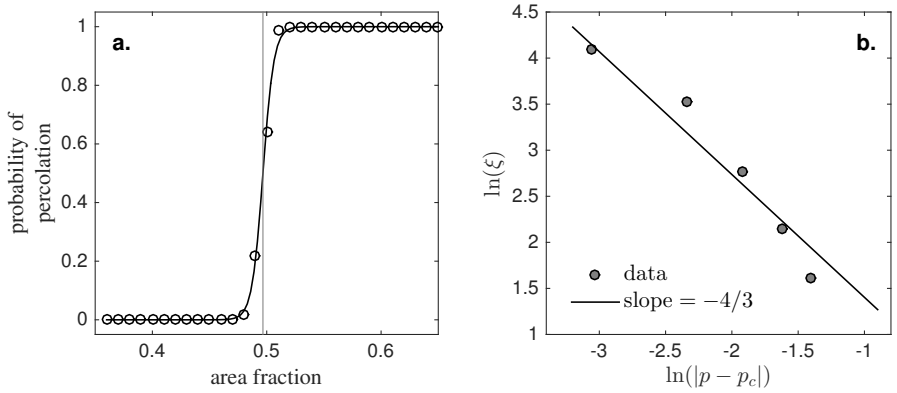

Supplementary Figure 3. (a) Probability of percolation as a function of area fraction. The curve is a hyperbolic tangent fit with inflection point close to 0.5 indicating the percolation threshold p_c. (b) Comparison of output from the Ising model (filled circles) to the line with slope $-\nu = -4/3$ given by the universal correlation length exponent ν.

where $\xi(p)$ is referred to as the correlation length. Theory indicates that $\xi(p)$ should obey

$$\ln \xi(p) \sim -\nu \ln(|p - p_c|), \quad p \longrightarrow p_c^-, \tag{S3}$$

where $\nu = 4/3$ is the universal critical exponent in two dimensions and p_c is the percolation threshold. For the two-dimensional square site lattice, $p_c \approx 0.59274621$ [38]. For the RFIM, analysis of 5,000 model realizations on 1024×1024 lattices yields a value close to $p_c = 0.5$ (Fig. 3a), with correlation lengths aligning reasonably with the universal exponent $\nu = 4/3$ (Fig. 3b). This result indicates that the spatial correlation structure of melt ponds in this model is sufficiently short-ranged so that the system falls within a standard universality class [15].

Nonzero uniformly applied field. — Let us choose $H \neq 0$ and keep $J \to +\infty$ in the RFIM given by Eq. (2). Then the tiebreaker rule for a chosen site i changes to $s_i = +1$ if $h_i < H$, and $s_i = -1$ if $h_i > H$, which favors ice for $H < 0$ and water for $H > 0$. Here we only consider two limiting cases when the tiebreaker rule completely favors ice or water: (I) $0 \ll -H \ll J$; (II) $0 \ll H \ll J$. In these cases, the random field h_i does not affect the kinetics, so the RFIM reduces to the classical Ising model without disorder,

$$\mathcal{H} = -H \sum_i s_i - J \sum_{\langle i,j \rangle} s_i s_j. \tag{S4}$$

The corresponding metastable states are known as Wulff droplets [39]. In case (I) the up-spin clusters are more elongated, and the percolation threshold is below 0.5. In case (II) the up-spin clusters are more circular, and the percolation threshold is above 0.5. These geometrical features afforded by varying H (and possibly also J) provide additional prospects to describe detailed shapes of real melt pond patterns.

Alternative update rule and free energy. — Let us retain the RFIM update rule when a majority exists among the neighboring sites, but adopt the following tiebreaker

rule: the chosen site is updated to ice if its pre-melt ice height is larger than the average between the two neighboring ice sites, and water otherwise. For example, in Fig. 1(b) we require that $s_P = +1$ if $h_P < (h_B + h_C)/2$, and -1 otherwise. This new update rule can be restated as minimizing an interfacial energy between water and ice: if a water site i neighbors an ice site j, then a penalty $W - h_j$ is imposed, where $W \gg 0$ is a constant. The total free energy $\mathcal{H}$ can then be written in two equivalent forms,

$$\mathcal{H} = \sum_{\langle i,j\rangle : s_i>0,\, s_j<0} (W - h_j) \equiv \sum_i s_i \Delta_i h - \sum_{\langle i,j\rangle} \frac{1}{2} s_i s_j (W - \Omega_{ij} h), \tag{S5}$$

where Δ_i and Ω_{ij} represent, respectively, the discrete Laplacian at site i and the average between sites i, j,

$$\Delta_i h \equiv h_i - \frac{1}{4} \sum_{j:\langle i,j\rangle} h_j, \quad \Omega_{ij} h \equiv \frac{1}{2}(h_i + h_j). \tag{S6}$$

The new "effective" random fields $\Delta_i h$, being the curvature of h_i, are more correlated than the h_i by themselves. As a result, at output pond fraction $F_{out} = 0.45$, the critical area for the transition in fractal dimension and the critical area for maximum elasticity are both $A_c a^2 \approx 120$ m^2. The corresponding power law scaling exponent for the pond size distribution is $\zeta = -1.57 \pm 0.03$.

References

[35] C. Petrich, H. Eicken, C. M. Polashenski, M. Sturm, J. P. Harbeck, D. K. Perovich, and D. C. Finnegan. Snow dunes: A controlling factor of melt pond distribution on Arctic sea ice. *J. Geophys. Res.*, 117:C09029, 2012.

[36] M. Sturm, J. Holmgren, and D. K. Perovich. Winter snow cover on the sea ice of the Arctic Ocean at the Surface Heat Budget of the Arctic Ocean (SHEBA): Temporal evolution and spatial variability. *J. Geophys. Res.*, 107(C10):C000400, 2002.

[37] D. L. Gilman, F. J. Fuglister, and J. M. Mitchell. On the power spectrum of red noise. *J. Atmos. Sci.*, 20(2):182–184, 1963.

[38] M. E. J. Newman and R. M. Ziff. Efficient Monte Carlo algorithm and high-precision results for percolation. *Phys. Rev. Lett.*, 85:4104–4107, 2000.

[39] R. H. Schonmann and S. B. Shlosman. Wulff droplets and the metastable relaxation of kinetic Ising models. *Commun. Math. Phys.*, 194(2):389–462, 1998.